Supporting Information for

Highly selective and active NO reduction to synthesize NH_3 based on graphene-substituted phthalocyanine Cu electrocatalysts

Jiaxiao Bai[a, b], Song Liu[*, a], Kuo Liu[*, b]

[a] College of Chemistry, Chemical Engineering and Resource Utilization, Northeast Forestry University, Harbin 150040, China

[b] Beijing Key Laboratory of Ionic Liquids Clean Process, Institute of Process Engineering, Chinese Academy of Sciences, Innovation Academy for Green Manufacture, Chinese Academy of Sciences, Beijing 100190, China

[*] Corresponding authors. E-mails: liusongcid@163.com (Song Liu), kuoliu@ipe.ac.cn (Kuo Liu)

Experimental details

1. Instrumentation

SEM images were obtained with a scanning electron microscope (SEM, JSM-6700F) operated at 5 kV.

Aberration-corrected high-angle annular dark-field scanning transmission electron microscopy (AC-STEM) images were recorded using a JEOL-ARM200F probe-corrected scanning/transmission electron microscope. Before AC-STEM experiments, a minimal quantity of the sample was dispersed in ethanol within a sample tube, and the resulting suspension was subjected to ultrasonic treatment for 30 minutes to achieve homogeneous dispersion. Subsequently, a small aliquot of the suspension was drop-coated onto a copper grid, followed by the AC-STEM study.

X-ray diffraction (XRD) data were collected using a Rigaku SmartLab 9 kW.

The absorbance data were measured on a UV-Vis spectrophotometer (Techcomp, UV2510).

ICP-OES (Atom scan Advantage, Avio 200, USA) was used to determine the content of Cu.

X-ray photoelectron spectroscopy was conducted using AXIS SUPRA+.

The Raman spectroscopy data were obtained from Renishaw inVia Qontor.

The Fourier transform infrared (FTIR) study were carried out on a Fourier transform infrared spectrometer (Bruker INVENIO S). A 5 mg sample was weighed and mixed with 500 mg of KCl (AR, Aladdin). The mixture was thoroughly ground and homogenized using a mortar and pestle to ensure uniform distribution. Subsequently, the blended powder was compressed into a pellet before FTIR analysis.

Attenuated total reflection Flourier transformed infrared spectroscopy (ATR-FTIR) was carried out by Fourier transform infrared spectrometer (Bruker INVENIO S). The catalyst was deposited onto the surface of a gold-coated silicon crystal, and the reference electrode was Ag/AgCl, while the counter electrode was a Pt wire. During the chronoamperometry measurements, spectral data were collected from -0.23 to -1.23 V vs. RHE by increasing the potential 100 mV each time.

The NO adsorption amounts were studied by NO-TPD using an Antaris IGS gas analyzer (Thermo Fisher Scientific, USA)[1]. In the NO-TPD test, 100 mg of the catalyst was weighed and subsequently placed within the reaction tube. The catalyst was then subjected to a pretreatment in Ar at 150 °C for 1 h. Afterwards, the reaction tube was allowed to cool to a temperature of 50 °C. Then, the catalyst was treated in a mixture of 1 vol% NO and Ar for one hour, followed by the removal of residual NO using Ar purging for one hour. Finally, the catalyst was heated to a temperature of 700 °C at a rate of 10 °C/min under an Ar atmosphere, with the gas composition detected with an IGS gas detector.

2. Synthesis of Cu/CG and Cu/GO

Anhydrous copper chloride (20 mg, AR, Macklin), trimeric anhydride (TMB, 60 mg, AR, Aladdin), carboxylated graphene (CG, 200 mg, ≥98 %, Leyan), and ammonium molybdate (40 mg, AR, Aladdin) were thoroughly ground in a mortar to achieve a uniform mixture. The resulting powder was transferred to a beaker and heated to 150 °C, followed by the slow addition of 0.8 g urea (AR, Macklin) under continuous stirring until complete melting of urea and dissolution of other reactants. Then the mixture was maintained at this temperature for 1 h before the temperature was gradually increased to 200 °C. Upon solidification, the mixture was transferred to an oven and maintained at 200 °C for an additional 1 h, and then cooled and ground into fine powder. Subsequently, the obtained material was subjected to reflux in 2 M hydrochloric acid (AR, Sinopharm Chemical Reagent) for 24 h, followed by hot filtration. The solid residue was washed with deionized water until the filtrate reached neutral pH, and then further rinsed with ethanol and dried under vacuum at 120 °C. The dried material was then dispersed in a 20% KOH (AR, Aladdin) solution and refluxed at 100 °C for 20 h. After cooling to room temperature, the mixture was acidified with concentrated hydrochloric acid to pH 2–3, filtered, washed until the pH value was neutral, and then dried. The resulting solid was dissolved in 1 M KOH solution, filtered, and the filtrate was adjusted to pH 2–3 using hydrochloric acid. Finally, the solid product was washed with ethanol and dried under vacuum at 100 °C, and then, Cu/CG was obtained.

For comparison, Cu/GO with the same copper content was synthesized. Anhydrous copper chloride (20 mg), trimeric anhydride (TMB, 60 mg), graphene oxide (GO, 200 mg, ≥98 %, XFNANO) and ammonium molybdate (40 mg) were thoroughly ground in a mortar to achieve a uniform mixture. The following steps were consistent with those of the Cu/CG preparation process.

3. Electrochemical parameters

Electrochemical tests were performed using a Koester electrochemical workstation. Cu/CG was employed as the working electrode, with Ag/AgCl as the reference electrode and converted to the RHE reference scale by E (vs. RHE) = E (vs. Ag/AgCl) + 0.197 V + 0.0591 × pH, and a Pt sheet as the counter electrode, forming a standard three-electrode system to evaluate the electrochemical performance. Ar gas was delivered into the cathodic compartment at a rate of 40 mL min^{-1} to remove dissolved O_2.

4. The calculation method for FE_{NH3}

The FE for NH_3 product was calculated at a given potential as follows:

$$FE_{NH3} = C_{NH3} \times V \times N \times F/(Q \times M)$$

where C_{NH3} is the measured mass concentration of product, V is the volume of the cathodic electrolyte, N is the number of electrons was needed to produce one product molecule, F is the Faraday constant (96485 C mol^{-1}), Q is the quantity of applied charge/electricity, and M is the relative molecular mass of specific product. The yield of NH_3 product (y_{NH3}) was calculated at a given potential as follows:

$$y_{NH3} = (C_{NH3} \times V)/(S \times t \times M)$$

where, t is the time for which the potential was applied and S is the geometric area of the working electrode.

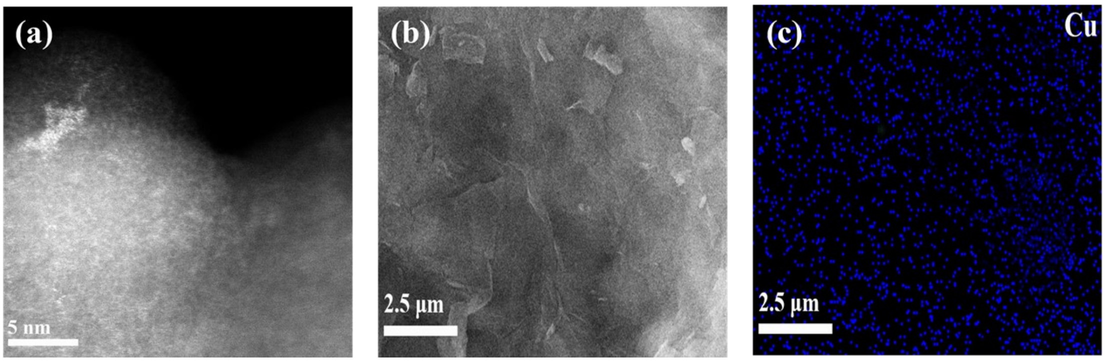

Fig. S1. (a) Typical AC-STEM, (b) SEM, and (c) Cu mapping images of Cu/GO.

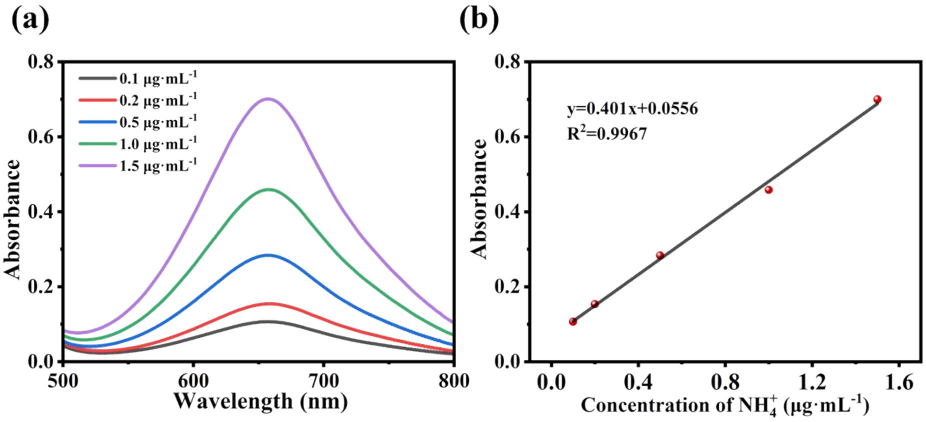

Fig. S2. (a) UV-Vis curves and (b) concentration-absorbance curve of NH_4^+ solution with a series of standard concentrations. The absorbance at 650 nm was measured by a UV-Vis spectrophotometer. The standard curve showed good linear relation of absorbance with NH_4^+ concentration ($y = 0.401x + 0.0556$, $R^2 = 0.9967$).

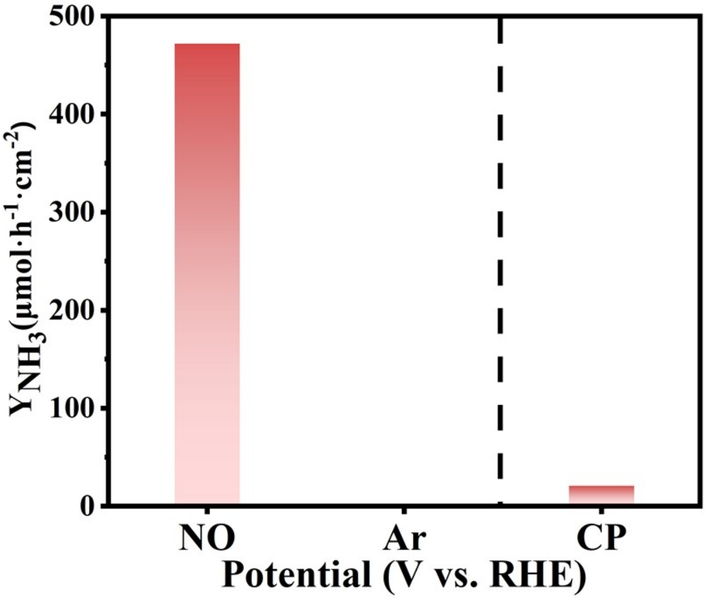

Fig. S3. NH_3 yield on Cu/CG and CP at various conditions.

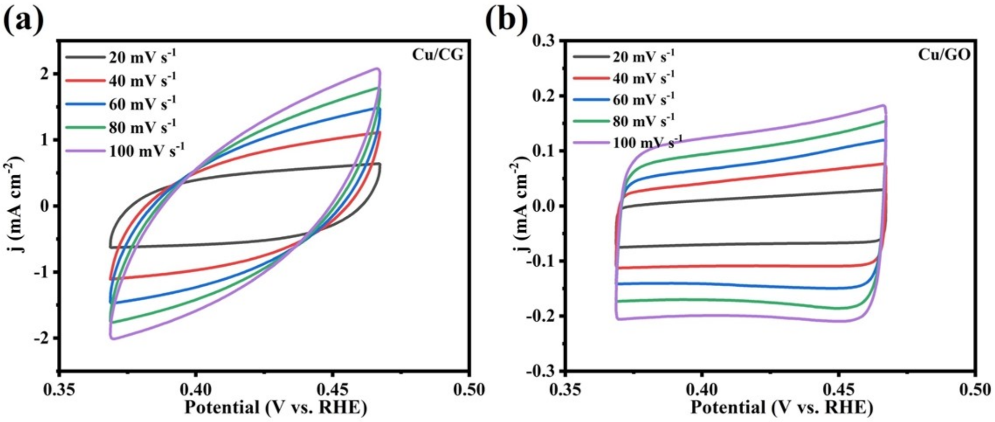

Fig. S4. CV curves for (a) Cu/CG and (b) Cu/GO.

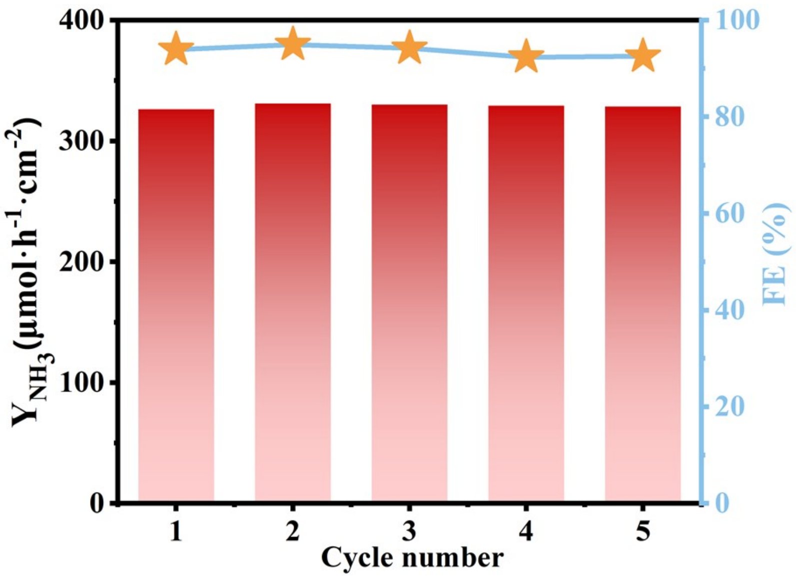

Fig. S5. Five-cycle stability test of Cu/CG.

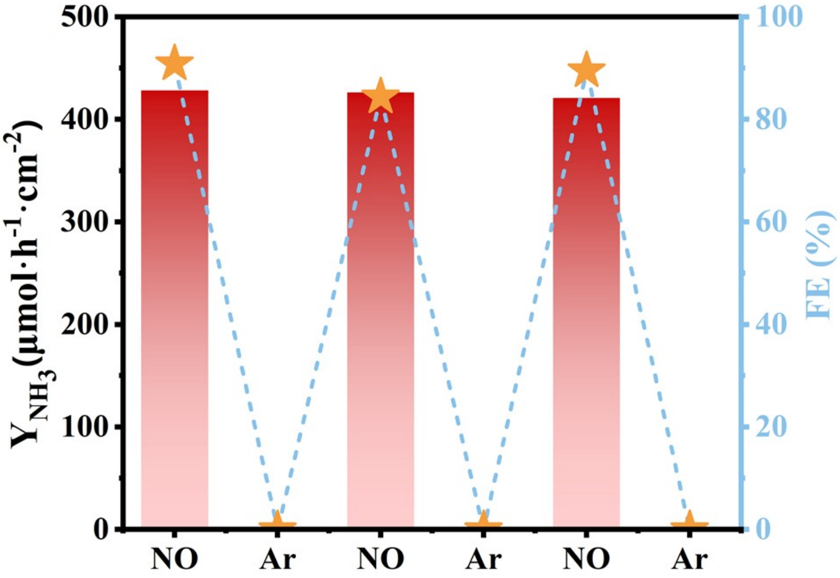

Fig. S6. NO-Ar alternating test for Cu/CG.

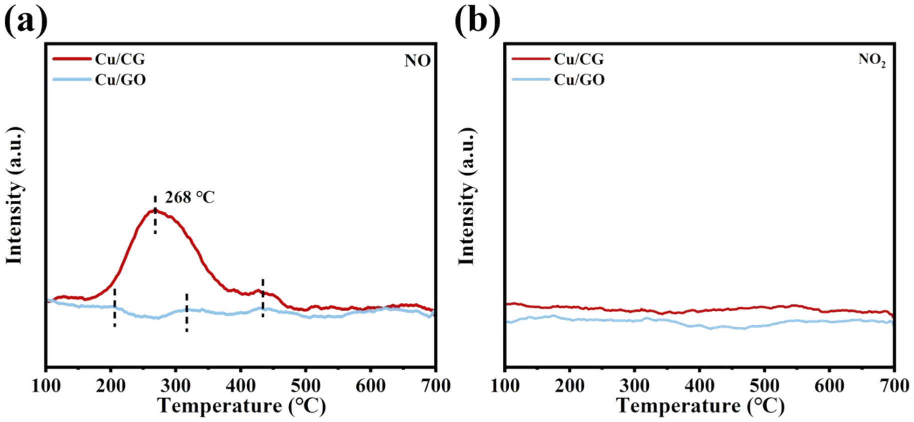

Fig. S7. (a) NO and (b) NO_2 evolution during the temperature-programmed desorption of NO (NO-TPD) on the Cu/CG and Cu/GO catalysts.

Table S1. ICP detection data of Cu content in Cu/CG and Cu/GO.

Catalysts	**Cu (%)**
Cu/CG	2.182336
Cu/GO	2.173031

Table S2. Comparison of Cu/CG with other catalysts in the literature.

Catalyst	**Electrolyte**	**Potential (V vs. RHE)**	**NH_3 yield**	**FE (%)**	**Ref.**
Cu/CG	0.1 M HCl	-1.2/-1.0	471.87 μmol·h^{-1}·cm^{-2}	94.07	This work
Ni_2P/CP	0.1 M HCl	-0.2	33.47 μmol·h^{-1}·cm^{-2}	76.9	2
$Ru_{0.05}Cu_{0.95}$	0.5 M Na_2SO_4	-0.49	17.68 μmol·h^{-1}·cm^{-2}	64.9	3
CoP/TM	0.2 M Na_2SO_4	-0.2	47.22 μmol·h^{-1}·cm^{-2}	88.3	4
FeP/CC	0.2 M PBS	-0.2	85.62 μmol·h^{-1}·cm^{-2}	88.49	5
Cu-Ti hollow fiber	0.05 M Na_2SO_4	-0.6	400 μmol·h^{-1}·cm^{-2}	90	6
HCNF/CP	0.2 M Na_2SO_4	-0.6	22.35 μmol·h^{-1}·cm^{-2}	88.33	7
NiNC@CF	0.5 M PBS	-0.5	94 μmol·h^{-1}·cm^{-2}	87	8
Ni@NC	0.1 M HCl	0.16	34.6 μmol·h^{-1}·cm^{-2}	72.3	9
MoS/GF	0.1 M HCl	-0.7/0.1	99.6 μmol·h^{-1}·cm^{-2}	76.6	10
Ru-LCN	0.5 M Na_2SO_4	-0.2	45.02 μmol·mg^{-1}·h^{-1}	65.96	11
Fe/C	0.5 M PBS /0.5 M H_2SO_4	-0.5	908 μmol·h^{-1}·cm^{-2}/ 1239 μmol·h^{-1}·cm^{-2}	77/ 50.4	12
CuFe DS/NC	0.1 M Na_2SO_4	-0.6	112.52 μmol cm^{-2}	90	13
hcp-Co	0.1 M Na_2SO_4	-0.6	439.50 μmol·h^{-1}·cm^{-2}	64.9	14
Cu foam	0.25 M Li_2SO_4	–0.9	517.1 μmol·h^{-1}·cm^{-2}	93.5	15
Cu foil	0.25 M Li_2SO_4	-0.9	95.0 μmol·h^{-1}·cm^{-2}	61.9	15

Catalyst	**Electrolyte**	**Potential (V vs. RHE)**	**NH_3 yield**	**FE (%)**	**Ref.**
Pt foil	0.25 M Li_2SO_4	-0.9	99.4 $\mu mol \cdot h^{-1} \cdot cm^{-2}$	24.1	15
CuFe-450	0.1 M PBS	–0.8	137.1 $\mu mol \cdot h^{-1} \cdot cm^{-2}$	90.6	16
CNNS/CP	0.1 M PBS	-0.8	30.7 $\mu mol \cdot h^{-1} \cdot cm^{-2}$	45.6	17
Cu_1/MoS_2	0.5 M Na_2SO_4	-0.6	337.5 $\mu mol \cdot h^{-1} \cdot cm^{-2}$	90.6	18
MnO_{2-x}NA/TM	0.2 M Na_2SO_4	–0.7	9.9 $\mu mol \cdot h^{-1} \cdot cm^{-2}$	82.8	19
Fe_1/MoS_{2-x}	0.5 M Na_2SO_4	-0.6	288.2 $\mu mol \cdot h^{-1} \cdot cm^{-2}$	82.5	20

Table S3. BET data of Cu/CG versus Cu/GO.

Catalyst	**BET Surface Area ($m^2 \cdot g^{-1}$)**	**t-Plot Micropore Area ($m^2 \cdot g^{-1}$)**	**t-Plot External Surface Area ($m^2 \cdot g^{-1}$)**
Cu/CG	15.6559	1.9155	13.7404
Cu/GO	18.5676	0.2317	18.3359

References:

1. K. Liu, H. He, Y. Yu, Z. Yan, W. Yang and W. Shan, *J. Catal.*, 2019, **369**, 372-381.

2. T. Mou, J. Liang, Z. Ma, L. Zhang, Y. Lin, T. Li, Q. Liu, Y. Luo, Y. Liu, S. Gao, H. Zhao, A. M. Asiri, D. Ma and X. Sun, *J. Mater. Chem. A*, 2021, **9**, 24268-24275.

3. J. Shi, C. Wang, R. Yang, F. Chen, N. Meng, Y. Yu and B. Zhang, *Sci. China: Chem.*, 2021, **64**, 1493-1497.

4. J. Liang, W.-F. Hu, B. Song, T. Mou, L. Zhang, Y. Luo, Q. Liu, A. A. Alshehri, M. S. Hamdy, L.-M. Yang and X. Sun, *Inorg. Chem. Front.*, 2022, **9**, 1366-1372.

5. J. Liang, Q. Zhou, T. Mou, H. Chen, L. Yue, Y. Luo, Q. Liu, M. S. Hamdy, A. A. Alshehri, F. Gong and X. Sun, *Nano Res.*, 2022, **15**, 4008-4013.

6. L. Chen, W. Sun, Z. Xu, M. Hao, B. Li, X. Liu, J. Ma, L. Wang, C. Li and W. Wang, *Ceram. Int.*, 2022, **48**, 21151-21161.

7. L. Ouyang, Q. Zhou, J. Liang, L. Zhang, L. Yue, Z. Li, J. Li, Y. Luo, Q. Liu, N. Li, B. Tang, A. Ali Alshehri, F. Gong and X. Sun, *J. Colloid Interface Sci.*, 2022, **616**, 261-267.

8. T. Muthusamy, S. Sethuram Markandaraj and S. Shanmugam, *J. Mater. Chem. A*, 2022, **10**, 6470-6474.

9. S. Sethuram Markandaraj, T. Muthusamy and S. Shanmugam, *Adv. Sci.*, 2022, **9**, 2201410.

10. L. Zhang, J. Liang, Y. Wang, T. Mou, Y. Lin, L. Yue, T. Li, Q. Liu, Y. Luo, N. Li, B. Tang, Y. Liu, S. Gao, A. A. Alshehri, X. Guo, D. Ma and X. Sun, *Angew. Chem., Int. Ed.*, 2021, **60**, 25263-25268.

11. Y. Li, C. Cheng, S. Han, Y. Huang, X. Du, B. Zhang and Y. Yu, *ACS Energy Lett.*, 2022, **7**, 1187-1194.

12. S. Cheon, W. J. Kim, D. Y. Kim, Y. Kwon and J.-I. Han, *ACS Energy Lett.*, 2022, **7**, 958-965.

13. D. Wang, X. Zhu, X. Tu, X. Zhang, C. Chen, X. Wei, Y. Li and S. Wang, *Adv. Mater.*, 2023, **35**, 2304646.

14. D. Wang, Z.-W. Chen, K. Gu, C. Chen, Y. Liu, X. Wei, C. V. Singh and S. Wang, *J. Am. Chem. Soc.*, 2023, **145**, 6899-6904.

15. J. Long, S. Chen, Y. Zhang, C. Guo, X. Fu, D. Deng and J. Xiao, *Angew. Chem., Int. Ed.*, 2020, **59**, 9711-9718.

16. R. Hao, L. Tian, C. Wang, L. Wang, Y. Liu, G. Wang, W. Li and G. A. Ozin, *Chem. Catalysis*, 2022, **2**, 622-638.

17. K. Li, Z. Shi, L. Wang, W. Wang, Y. Liu, H. Cheng, Y. Yang and L. Zhang, *J. Hazard. Mater.*, 2023, **448**, 130890.

18. K. Chen, G. Zhang, X. Li, X. Zhao and K. Chu, *Nano Res.*, 2023, **16**, 5857-5863.

19. Z. Li, J. Liang, Q. Liu, L. Xie, L. Zhang, Y. Ren, L. Yue, N. Li, B. Tang, A. A. Alshehri, M. S. Hamdy, Y. Luo, Q. Kong and X. Sun, *Mater. Today Phys.*, 2022, **23**, 100619.

20. K. Chen, J. Wang, J. Kang, X. Lu, X. Zhao and K. Chu, *Appl. Catal., B*, 2023, **324**, 122241.